

Advantages of Combined Use of Claw Hooks and Sublaminar Wires as the Upper Foundation of Long Fixation from the Thoracic Spine to the Pelvis in Osteoporotic Cases: A Finite Element Analysis of Proximal Junction Stress

Takuhei Kozaki¹⁾, Takachika Shimizu²⁾, Akimasa Murata¹⁾, Ryuichiro Nakanishi¹⁾, Takahiro Kozaki¹⁾, Ei Yamamoto³⁾, Shunji Tsutsui¹⁾, Mamoru Kawakami⁴⁾ and Hiroshi Yamada¹⁾

1) Department of Orthopaedic Surgery, Wakayama Medical University, Wakayama, Japan

2) Department of Orthopaedic Surgery, Gunma Spine Center (Harunaso Hospital), Takasaki, Japan

3) Department of Biomedical Engineering, Faculty of Biology-Oriented Science and Technology, Kindai University, Wakayama, Japan

4) Department of Orthopaedic Surgery, Saiseikai Wakayama Hospital, Wakayama, Japan

Abstract:

Introduction: This study aimed to compare the biomechanical stress at the proximal junctional aspect between the conventional pedicle screw (PS) fixation (PSF) and the low PS density fixation (LPF) method.

Methods: This study involved 10 patients, half of whom have non-osteoporosis and the other half have osteoporosis. We made two types of intact models (one is from the upper thoracic-to-pelvis model, and the other is from the lower thoracic-to-pelvis model). From the intact models, we constructed two kinds of fusion models: (1) PSF and (2) LPF. The LPF method was as follows: The claw hooks (the combination of the down-going transverse process hooks and facet hooks) were set at the upper instrumented vertebra (UIV) and sublaminar wires at the thoracic spine and PSs at the lumbo-pelvis.

Results: *Upper thoracic to pelvis fixation model*

In non-osteoporosis, no significant difference between the PSF and LPF is found. In osteoporosis, the von Mises stresses of the vertebra body at UIV, UIV+1, and disc were significantly lower in LPF than in PSF.

Lower thoracic-to-pelvis fixation model

In non-osteoporosis, the average von Mises stress of the vertebral body at UIV+1 and the maximum stress at UIV were lower in LPF than in PSF; however, no significant difference was found in the others. In osteoporosis, the von Mises stress was significantly lower in LPF than in PSF.

Conclusions: The claw hooks stabilized the vertebra body at UIV firmly, and sublaminar wires reduced load translation from the fixed spine.

Keywords:

low pedicle screw density fixation, thoracic claw hooks, sublaminar wires, osteoporosis, proximal junctional kyphosis, finite element analysis

Spine Surg Relat Res 2025; 9(2): 202-210
dx.doi.org/10.22603/ssrr.2024-0169

Introduction

In the aging population, adult spinal deformity (ASD) has become one of the most common spinal disorders. It has a possibility of low back pain and interferes with daily activities. The quality of life of patients with ASD has been en-

hanced through surgical treatments, but these are complex because of the complex nature of several types of complications. At the present time, proximal junctional kyphosis (PJK) has become a common problem after spinal fusion surgery¹⁾. Reportedly, the incidence of PJK is high²⁻⁴⁾. This pathology is derived from degenerative changes at the proxi-

Corresponding author: Takachika Shimizu, tshimizu@dan.wind.ne.jp

Received: June 12, 2024, Accepted: July 10, 2024, Advance Publication: August 30, 2024

Copyright © 2025 The Japanese Society for Spine Surgery and Related Research

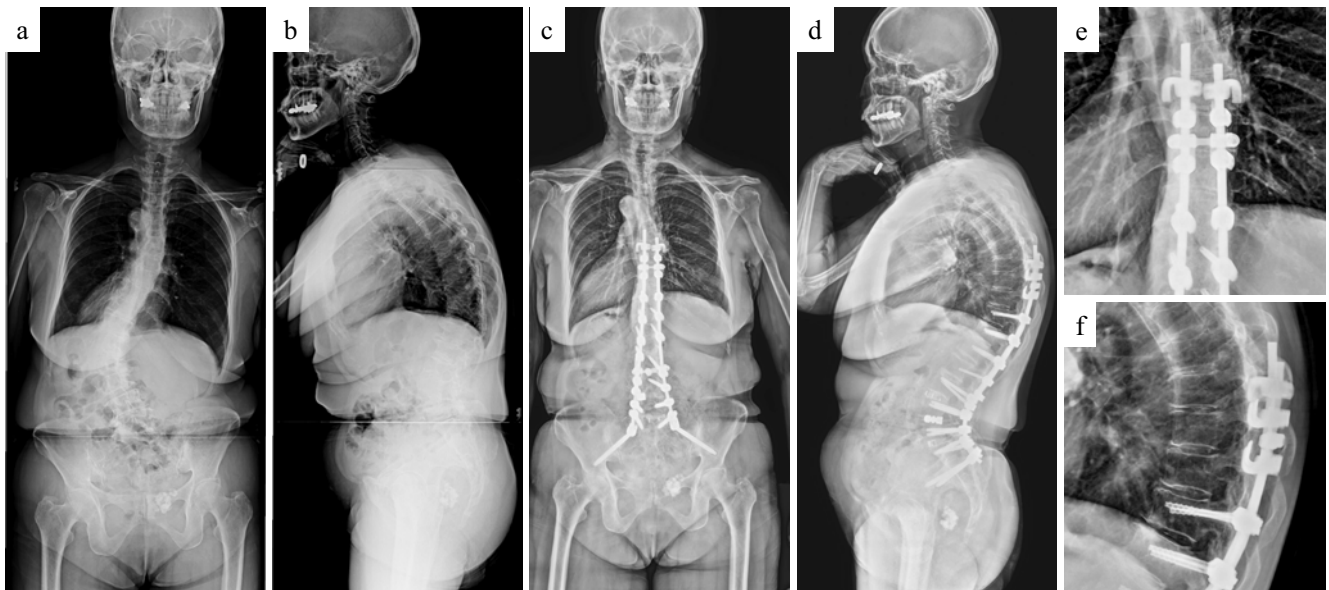


Figure 1. A 68-year-old female underwent spinopelvic fusion surgery for kyphoscoliosis using multiple hooks (a, b). Three years later, the alignments were preserved, and no implant failure was observed (c, d). The upper foundation of this case was claw hooks (down-going transverse process hooks and facet hooks) at T9 and facet hooks at T10 (e, f).

mal aspect adjacent to the fused segments^{5,6}. PJK is still a challenging problem that decreases patients' functional outcomes and leads to further surgical interventions⁷⁻⁹. Hence, to maintain good radiological and clinical outcomes, mechanical complications must be resolved.

Based on previous literature, PJK is likely to be a multifactorial phenomenon that includes advanced age at surgery, female sex, the presence of osteoporosis, spinal alignment, and excessive deformity correction¹⁰⁻¹². The placement of transverse process hooks (TPHs) in the uppermost instrumented vertebra (UIV) has often been discussed to be one of the techniques for the prevention of PJK/proximal junctional failure (PJF) and support pedicle screws (PSs)¹³⁻¹⁵, but this method has not fully achieved the goal. A biomechanical study revealed that a less rigid fixation at the proximal aspect reduces the risk of PJK by allowing less load transmission from the fused spine to the next mobile segments^{16,17}. Conversely, recent clinical studies reported that TPHs were associated with a significantly higher incidence of PJK than PSs during fusion surgery from the lower thoracic spine to the pelvis^{18,19}. This is because the lower part of the thoracic spine, which is only supported by false or floating ribs, is biomechanically more vulnerable than the upper and middle parts²⁰.

Despite that the placement of down-going TPHs in UIV has often been discussed to be one of the techniques to prevent PJK/PJF or to support PSs, we believed that this was insufficient in terms of mechanical strength²¹. Thus, we have considered the following method as the uppermost foundation: claw hooks in UIV and facet hooks in UIV-1 (Fig. 1)²². No mechanical studies on this upper foundation model in long stabilization from the thoracic spine to the pelvis were found. This study aimed to compare the biomechanical stress at the proximal junctional aspect between all pedicle

screw construct and the uppermost claw hooks fixation method.

Materials and Methods

The ethics committee of our institution approved this study, in which 10 patients were involved. Half of them had osteoporosis, and the other half had non-osteoporosis (Table 1). Patients were divided into two groups based on the T-score of the femoral neck given that the spine lesion has several spondylosis changes (osteophyte or bone sclerosis) and the possibility of overestimation of bone mineral density. When (1) the T-score was -2.5 or less or (2) if patients had a history of osteoporotic vertebral fractures, the patients were defined as osteoporotic. The others were non-osteoporotic. Using images generated via computed tomography (CT), a three-dimensional nonlinear finite element (FE) model was established. CT was taken from the cervical spine to the lower limb via simultaneous scanning of a calibration phantom (BMAS 200; Kyoto Kagaku, Kyoto, Japan), containing hydroxyapatite rods to determine bone density.

FE models were constructed from the patients' DICOM CT data and analyzed using Mechanical Finder[®] software version 12 (RCCM, Tokyo, Japan). An FE model from the spine to the pelvic bone was equipped with 2-mm tetrahedral solid elements. Based on previous reports, the lumbar spine²³ was adopted. Young's modulus, E , for bone in the pelvis, femur, and lumbar spine was determined from bone density (ρ) using the equations below, as proposed in a previous study²⁴:

$$E=0.01 \text{ (if } \rho=0\text{),}$$

$$E=33900\rho^{2.20} \text{ (if } 0<\rho\leq0.27\text{),}$$

$$E=5307\rho+469 \text{ (if } 0.27<\rho<0.6\text{),}$$

Table 1. Characteristics of the Subjects.

| | Non-osteoporosis | Osteoporosis | p-value |
|--|------------------|--------------|---------|
| Age (years old) | 64.0±16.4 | 74.8±3.1 | 0.60 |
| Male/female | 4/1 | 0/5 | 0.0036 |
| Body mass index (kg/m ²) | 27.2±9.1 | 22.3±2.5 | 0.68 |
| Bone mineral density (mg/cm ²) | 1024.8±54.1 | 631.2±164.8 | 0.016 |
| T-score | 0.080±0.69 | -2.42±1.2 | 0.036 |

Table 2. Material Properties.

| Material | Stiffness coefficient (N/mm) | Elements |
|---------------------------------------|-------------------------------------|----------|
| Anterior longitudinal ligament | 0 (ε<0), 49.7 (ε<12), 127.4 (12<ε) | Truss |
| Posterior longitudinal ligament | 0 (ε<0), 20.0 (ε<11), 40.0 (11<ε) | Truss |
| Ligamentum flavum | 0 (ε<0), 60.0 (ε<6.2), 78.0 (6.2<ε) | Truss |
| Transverse ligament | 0 (ε<0), 1.8 (ε<18), 10.6 (18<ε) | Truss |
| Capsular ligament | 0 (ε<0), 22.5 (ε<25), 98.7 (25<ε) | Truss |
| Interspinous ligament | 0 (ε<0), 40.0 (ε<14), 46.4 (14<ε) | Truss |
| Supraspinous ligament | 0 (ε<0), 19.2 (ε<20), 48.0 (20<ε) | Truss |
| Sacrospinous ligament | 1400 | Truss |
| Sacroterous ligament | 1500 | Truss |
| Interosseous ligament | 2800 | Truss |
| Sacroiliac anterior ligament | 700 | Truss |
| Sacroiliac posterior ligament (short) | 400 | Truss |
| Sacroiliac posterior ligament (long) | 1000 | Truss |
| Iliolumbar ligament | 1000 | Truss |
| Pubic superior ligament | 500 | Truss |
| Pubis arcuate ligament | 500 | Truss |
| sublaminar wire | 661 | Truss |

| Material | Elastic modulus (MPa) | Poisson's ration |
|--------------------------|-----------------------|------------------|
| Fibrous rings | 450 | 0.45 |
| Vertebral pulp | 2.25 | 0.4995 |
| Sacrum cartilage | 54 | 0.4 |
| Pubic symphysis | 5 | 0.45 |
| Implant (titanium alloy) | 110000 | 0.3 |

$E=10200\rho^{2.01}$ (if $0.6\leq\rho$).

Poisson's ratio was 0.40. To calculate bone density from CT values (in Hounsfield units, HU), the following set of equations was employed:

ρ (g/cm³)=(CT number+1.4246)×0.001/1.058 (if CT number>-1 HU)

ρ (g/cm³)=0 (if CT number≤-1 HU)

Table 2 lists the material properties of soft tissues, ligaments, muscles, and sublaminar wires²⁵⁻²⁷.

FE model: validation

The lumbar spine functionally was validated based on previous research²⁸. The experimental study simulated motions of the following: flexion, extension, axial rotation, and lateral bending. The sacrum was constrained, and an L1-sacrum model was utilized. The range of motions of the flexion, extension, axial rotation, and lateral bending were favorably compared with that in the previous experimental study (Fig. 2).

From the intact model, we constructed two types of fixation models: (1) all PS fixation models (PSF) and (2) low PS density fixation (LPF) models, in which multiple hooks are placed in UIV. Three-dimensional models of the PSs (titanium alloy) and hooks (titanium alloy) were made from micro-CT data. The rods (diameter 5.5 mm, titanium alloy) were modeled using Metasequoia[®] version 4 (Tetraface, Tokyo, Japan). The PS, hook, and rod models were then meshed in Mechanical Finder. We created the upper thoracic-to-pelvis fixation model (Fig. 3) and the lower thoracic-to-pelvis fixation model (Fig. 4).

Upper thoracic-to-pelvis fixation model (Fig. 3)

In the PSF model, PSs were set from T2 to S1 with S2 alar iliac (AI) screw fixation. Each screw occupied more than 80% of the vertebra. In the LPF model, the bilateral claw hooks (the combination of the bilateral down-going TPHs and facet hooks) were set at T2 (UIV), facet hooks at T3 (UIV-1), sublaminar wires at T4-L1, and PSs at L2-S1

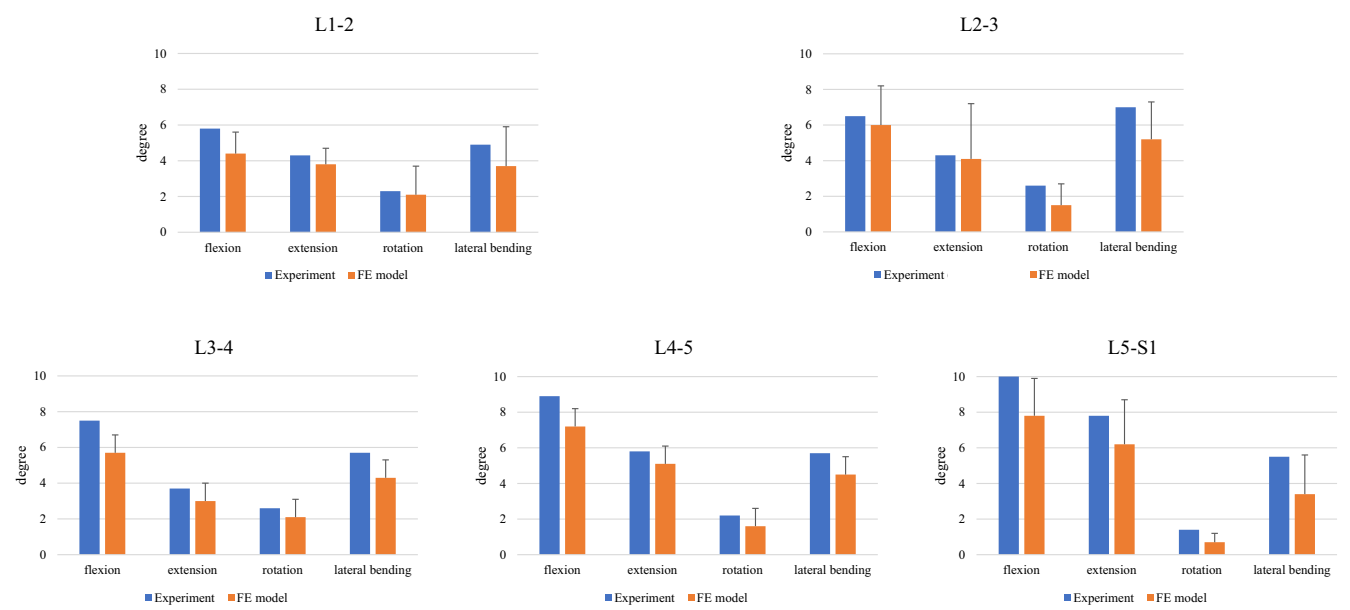


Figure 2. The range of motion of the lumbar spine of our finite element (FE) models was validated with a previous study.

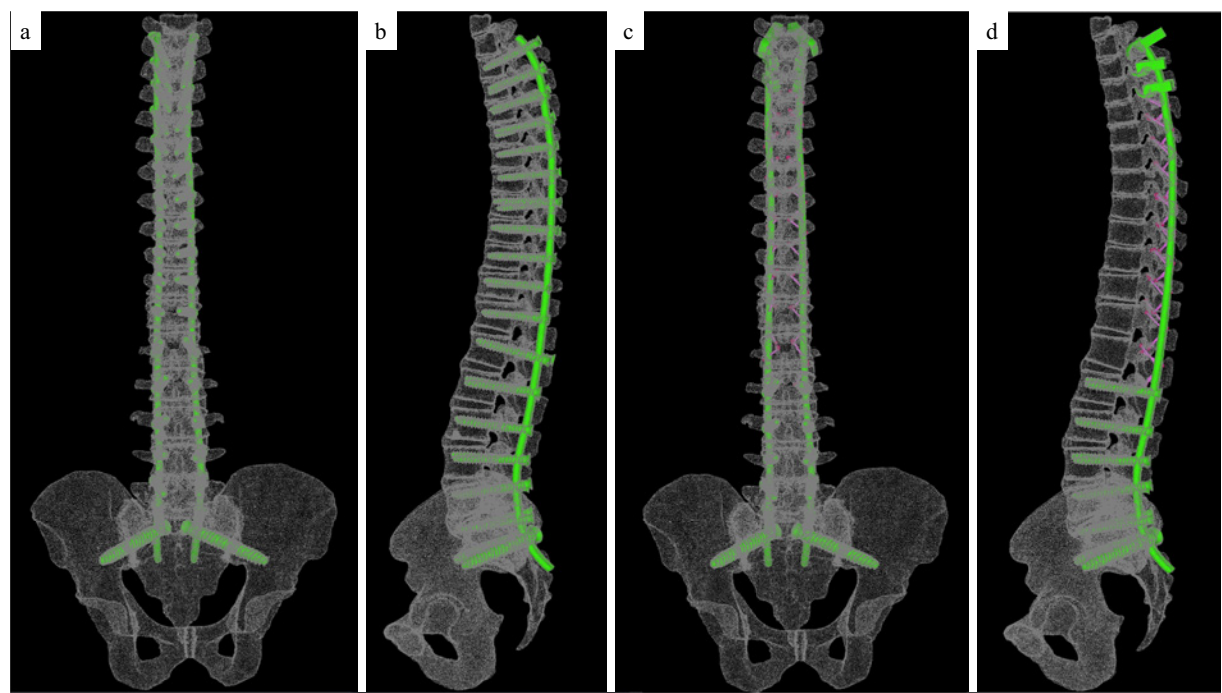


Figure 3. Upper thoracic spine to pelvis fixation model by all pedicle screw fixation (a, b) and low pedicle screw density fixation (c, d).

with S2 AI screw fixation. The blade of the facet hook was inserted into the facet joint from the caudal end of the inferior articular process and reached the inferior aspect of the pedicle. The down-going TPH was placed as close to the base of the TP as possible to avoid breaking the TP²¹⁾. The sublaminar wire was designed as truss elements divided into two segments and attached to the lamina, as described in the previous study²⁸⁾ (Fig. 5a, b).

Lower thoracic-to-pelvis fixation model (Fig. 4)

We created the lower thoracic-to-pelvis fixation model. In the PSF method, the PSs were set from T10 to S1 with S2

AI screw fixation. In the LPF method, the claw hooks (the combination of the bilateral down-going TPHs and facet hooks) were set at T10 (UIV), sublaminar wires at T11-T12, and PSs at L1-S1 with S2 AI screw fixation (Fig. 5c).

Analysis

We applied 100 N at the upper endplate of the C7 vertebra, followed by the 10-Nm flexion moment in the upper thoracic-to-pelvis fixation model. We applied 400 N at the upper endplate of the T8 vertebra, followed by the 10-Nm flexion moment in the lower thoracic-to-pelvis fixation model. The contact conditions were defined on the interfaces

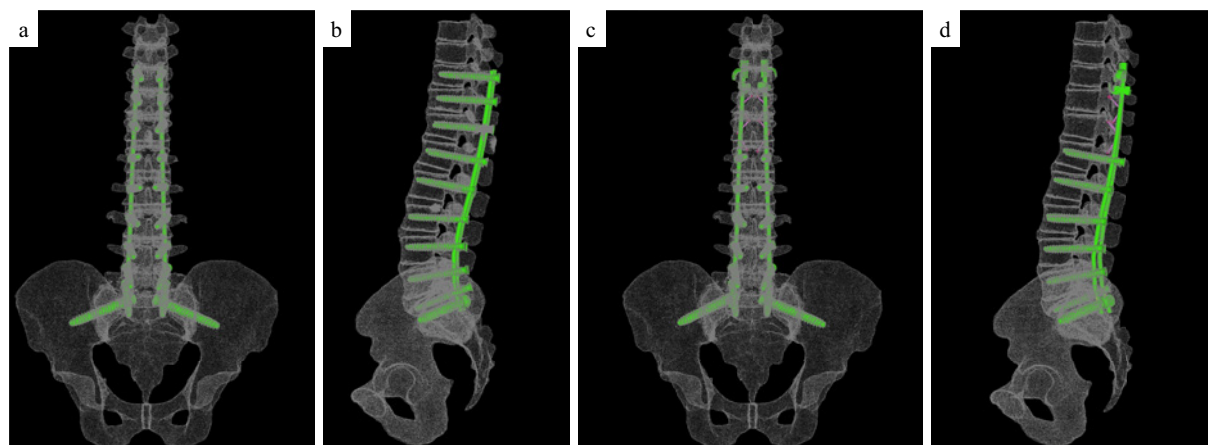


Figure 4. Lower thoracic spine to pelvis fixation model by pedicle screw fixation (a, b) and low pedicle screw density fixation (c, d).

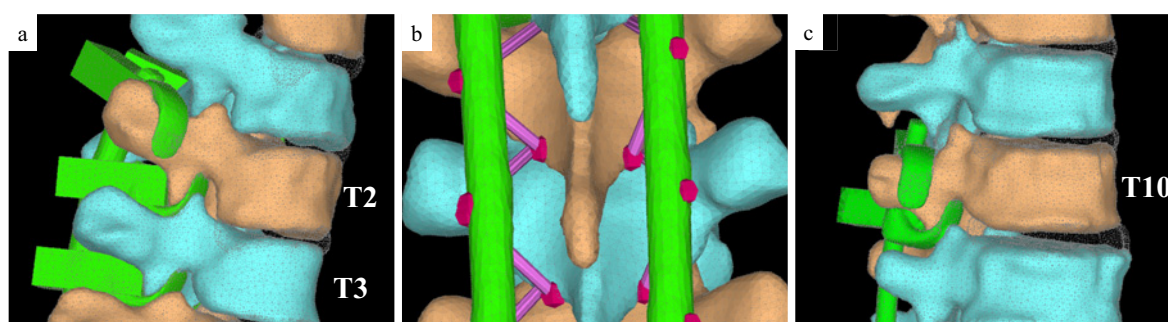


Figure 5. The setting of the claw hooks (the combination of the bilateral down-going transverse hooks and facet hooks) at T2, facet hooks at T3 (a), and sublaminar wires (b) from T4 to L1 in the upper thoracic spine to pelvis fixation model. The setting of claw hooks at T10 (c) and sublaminar wires from T11 to T12 in the lower thoracic spine to pelvis fixation model.

of PSs at UIV to the vertebral bone in the PSF model and interfaces of all hooks to the vertebral bone in the LPF model. The friction coefficient on the contact surfaces was set to 0.0. We analyzed the von Mises stress at the ventral half of the vertebral body at UIV, UIV+1, and the disc at UIV/UIV+1.

Statistical analysis

All numerical data are expressed as mean±standard deviation. Paired Student's *t* test was employed for statistical comparison, and the criterion for statistical significance was $p < 0.05$.

Results (Table 3)

Upper thoracic-to-pelvis fixation model: Non-osteoporosis

No significant difference was found between PSF and LPF in the von Mises stress of the vertebra at UIV, UIV+1, and disc at UIV/UIV+1.

Upper thoracic-to-pelvis fixation model: Osteoporosis

The average and maximum von Mises stress of the vertebra body at UIV, UIV+1, and disc were significantly lower

in LPF than in PSF.

Lower thoracic-to-pelvis fixation model: Non-osteoporosis

The average von Mises stress of the vertebral body at UIV+1 was lower in LPF than in PSF. Moreover, the maximum von Mises stress of the vertebral body at UIV was lower in LPF than in PSF. The maximum von Mises stress of the vertebral body at UIV+1, and the average stress at UIV tended to be smaller in LPF than in PSF, but no significant differences were found. In the same condition, the average and maximum stress at the disc (UIV/UIV+1) had a smaller tendency in LPF than in PSF, but no significant differences were found.

Lower thoracic-to-pelvis fixation model: Osteoporosis

The average and maximum von Mises stress of the vertebra body at UIV, UIV+1, and disc were significantly lower in LPF than in PSF.

Representative case

In the upper thoracic-to-pelvis model without osteoporosis, the stress was concentrated around the pedicle and little at the vertebra side of UIV in PSF. Likewise, the stress worked at the hook sites and less at the vertebra side at T2

Table 3. The Von Mises Stress.

| | PSF | LPF | p-value |
|--|-----------|-----------|---------|
| Non-osteoporosis (upper thoracic to pelvis fixation model) | | | |
| average von Mises stress at UIV+1 | 3.6±1.5 | 3.3±1.2 | 0.085 |
| maximum von Mises stress at UIV+1 | 44.3±26.3 | 25.2±7.1 | 0.080 |
| average von Mises stress at UIV | 2.2±0.75 | 2.0±0.70 | 0.23 |
| maximum von Mises stress at UIV | 26.4±11.9 | 16.7±7.7 | 0.12 |
| average von Mises stress at disc | 2.2±1.5 | 2.8±2.3 | 0.65 |
| maximum von Mises stress at disc | 12.0±8.8 | 9.3±5.4 | 0.32 |
| Osteoporosis (upper thoracic to pelvis fixation model) | | | |
| average von Mises stress at UIV+1 | 5.3±0.80 | 3.7±1.3 | 0.01 |
| maximum von Mises stress at UIV+1 | 39.2±10.2 | 26.8±8.6 | 0.047 |
| average von Mises stress at UIV | 3.8±0.43 | 2.3±0.51 | 0.0034 |
| maximum von Mises stress at UIV | 87.1±19.8 | 23.8±7.9 | 0.0006 |
| average von Mises stress at disc | 3.1±0.58 | 1.8±0.49 | 0.013 |
| maximum von Mises stress at disc | 18.2±10.3 | 8.6±2.9 | 0.049 |
| Non-Osteoporosis (lower thoracic to pelvis fixation model) | | | |
| average von Mises stress at UIV+1 | 2.4±0.29 | 1.9±0.26 | 0.0014 |
| maximum von Mises stress at UIV+1 | 16.8±7.9 | 11.8±2.6 | 0.15 |
| average von Mises stress at UIV | 1.4±0.52 | 1.4±0.57 | 0.57 |
| maximum von Mises stress at UIV | 22.2±13.8 | 8.4±3.4 | 0.024 |
| average von Mises stress at disc | 0.89±0.33 | 0.69±0.24 | 0.071 |
| maximum von Mises stress at disc | 5.3±4.1 | 3.0±0.83 | 0.17 |
| Osteoporosis (lower thoracic to pelvis fixation model) | | | |
| average von Mises stress at UIV+1 | 2.7±0.56 | 1.7±0.35 | 0.014 |
| maximum von Mises stress at UIV+1 | 38.5±18.2 | 21.5±3.7 | 0.042 |
| average von Mises stress at UIV | 2.2±0.56 | 1.4±0.36 | 0.043 |
| maximum von Mises stress at UIV | 49.0±10.5 | 18.5±8.6 | 0.0037 |
| average von Mises stress at disc | 1.5±0.65 | 0.92±0.51 | 0.013 |
| maximum von Mises stress at disc | 7.4±3.9 | 4.0±2.6 | 0.046 |

UIV, upper instrumented vertebra

in LPF. In the osteoporosis model, the stress worked both around the pedicle and the vertebra side at T2 around the PSs in PSF, but the main stress was focused only on the hook sites and less on the vertebra side at T2 in LPF (Fig. 6).

Discussion

We examined the stress around the proximal junctional aspect in spinopelvic fusion and compared the conventional all PS fixation method and the combination of claw hooks at UIV, facet hooks at UIV-1, and sublaminar wire at the thoracic lesion. In the non-osteoporosis model, the stress around the PSs at UIV did not significantly differ from that around the LPF. However, in the osteoporosis model, the stress was increased more in the PSF than in the LPF. Any mechanical studies on this upper foundation model in long stabilization from the thoracic spine to the pelvis have not been found.

The PJK was a multifactorial phenomenon. The trajectory of PSs might affect the occurrence of PJK. The past study revealed that straightforward insertion of PSs was superior to the anatomical trajectory in the thoracic spine¹⁹. PJK more frequently occurs in the presence of multiple cobalt-

chrome rods than in two titanium alloy rods²⁹. Implant-related complications, such as PS loosening or loss of the correction under osteoporotic bone must be prevented, especially around the UIV area³⁰. The prevention of PSs loosening has been reported in terms of screw thickness, insertion depth, angulation, pull-out strength, insertion torque, and bone mineral density^{31,32}. These factors significantly increased the stability of PSs in the non-osteoporotic vertebra, but the screw size had little or no effect on osteoporotic bone³³. The stability of the PSs was mainly influenced by the construct of the pedicle³⁰. In healthy vertebrae, the pedicle has sufficient strength to support the PSs, but osteoporosis weakens the cortical and cancellous bone of the pedicle, which cannot increase the stability of the PSs completely^{30,34}. These structural deficits may induce the micro-movement of the PSs and add stress to the vertebral body. It was shown that the vertebral body, while contributing two-thirds of the vertebral volume in the lumbar spine, only contributed one-third, on average of the bone mineral density, with the posterior elements contributing the remainder. It might be a disadvantage in fixing the osteoporotic spine in three dimensions^{35,36}. Conversely, the past paper noted that the resistance to failure in lamina hook and sublaminar wire fixation was not related to the bone mineral density^{34,37}. The

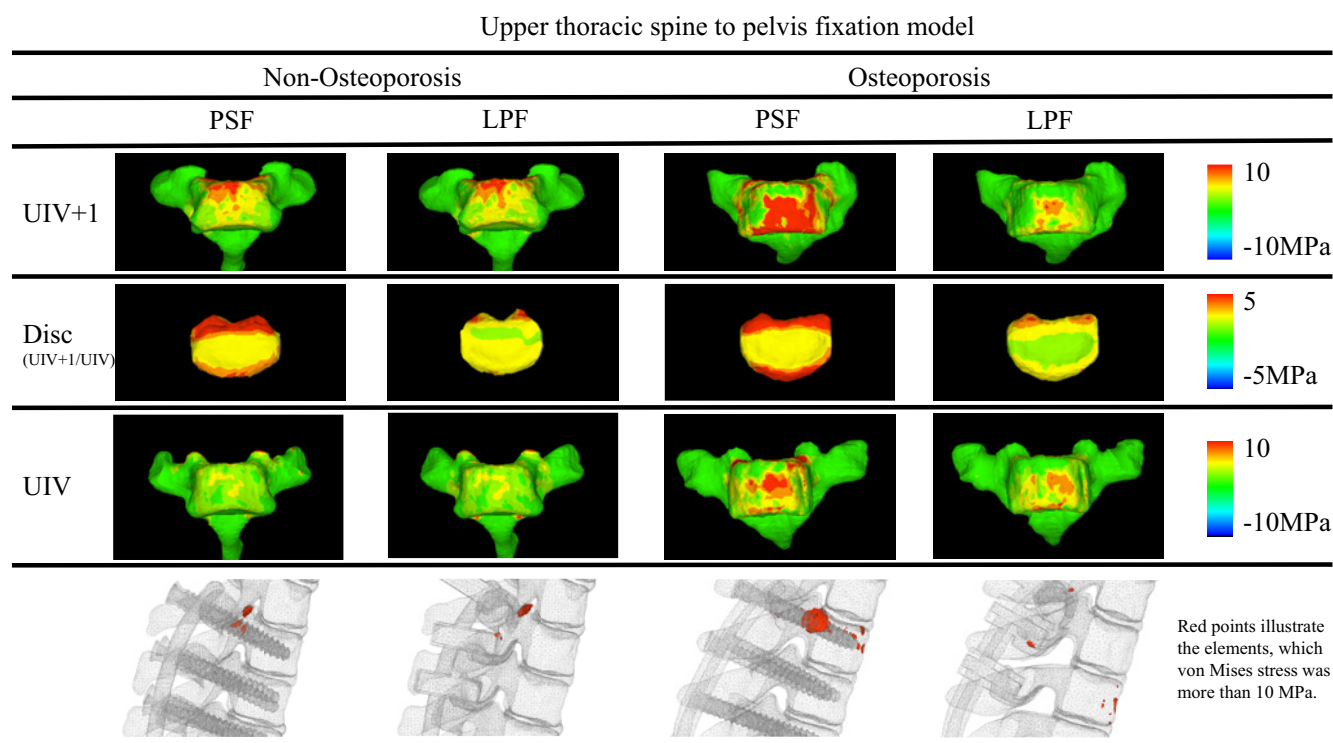


Figure 6. The view of the stress distribution in all pedicle screw fixation (PSF) model and low pedicle screw fixation (LPF) model. In osteoporosis, the stress concentration has occurred in the PSF but not in the LPF model. Conversely, in non-osteoporosis, the stress concentration has not made a difference between PSF and LPF.

combination of the PSs and facet hooks had greater resistance than the PS alone in osteoporotic bone³⁸). This might be because the inferior articular process and lamina have greater bone mineral density than the pedicle³⁵). We set the “claw hooks” as a combination of the inferior articular process hooks and down-going TPHs (Fig. 5a, c), which can firmly hold the posterior components of the vertebra in three dimensions and, at the same time, decrease the stress at the vertebral body. The multiple thoracic hooks at the end sites of the long fusion have good surgical results even in the fragile spine^{39,40}). Additionally, we believe that the hooks have less risk for additional neurological deficits via junctional problems than PSs in cases with backward pull-out of instrumentation³⁹⁻⁴¹).

This study also set the sublaminar wires in the thoracic-thoracolumbar lesion. Surgeons often apply the correction force through the implants at these lesions to correct the sagittal and coronal alignment, but these procedures have a risk of screw backout or fracture in an osteoporotic vertebra. The vertebral strength at the thoracolumbar lesion became weaker than the lumbar lesion⁴²), but previous studies show that osteoporosis has less impact on the strength of the sublaminar wiring^{34,37}). Moreover, the sublaminar wire has a good effect on the correction of scoliosis^{43,44}). Good correction of the scoliosis has been reported, even in the case of severe neurogenic scoliosis⁴⁵). The use of the sublaminar wires was less rigid fixation than all PS fixation and might relate to lower stress at the disc (UIV/UIV+1) and vertebra (UIV+1). Above them, the combination of the claw hooks

and sublaminar wires may induce the stability of the vertebra body (UIV) and reduce stress translation from the fixed segments to the adjacent mobile disc at UIV/UIV+1 and vertebra at UIV+1.

This study has several limitations. First is the small sample size. The female bone model had more patients in the osteoporosis group and had smaller pedicles, which might be related to the disadvantage of the PSs fixation. The models in this study were computed from Japanese subjects, who might have a smaller pelvic incidence than Western populations. The larger pelvic incidence and lumbar lordosis were related to the mechanical complication^{46,47}). A following study including Western subjects with higher pelvic incidence should be carried out in the future. Second, the contact surface between the PS and bone surface was simulated as completely fused except for PSs at UIV and all hooks, because the capacity of the computer processing power was limited. Finally, mechanical stress was applied in the forward bending direction only at the UIV+2. PJK could result from various factors, including fracture at the UIV and/or UIV±1 and the adjacent intervertebral segments. Additionally, these models did not include the rib cage. Further biomechanical studies using FE analysis, including the whole spine and rib cage, based on patients with ASD and/or cadaveric bone in the laboratory, should be conducted to reveal an ideal construct to avoid mechanical complications.

Conclusions

This study revealed that a combination of the multiple hooks and sublaminar wires decreased the stress at the UIV, UIV+1, and disc at UIV/UIV+1 in the osteoporosis model. It was believed that in this mechanism, the claw hooks stabilized the vertebra at UIV in three dimensions and reduced load transfer from the fixed spine by the combined use of sublaminar wires. This method may have an advantage in terms of prevention of proximal junctional problems, especially in osteoporosis cases.

Conflicts of Interest: The authors declare that there are no relevant conflicts of interest.

Sources of Funding: Not applicable.

Acknowledgement: We express our sincere gratitude to the late Mr. Hiroshi Yamada, the founder of Canopus, Co., Ltd., for their support and funding.

Author Contributions: T.K. and S.T. designed the study; T.K., A.M., R.N., and T.K. performed the experiments and analyzed the data; E.Y., S.T., M.K., and H.Y. supervised the experiments; T.K. and T.S. wrote the manuscript.

Ethical Approval: This study was approved by an Institutional Review Board of Wakayama Medical University (No. 2511).

Informed Consent: The patient provided informed consent to participate in and publish this study.

Availability of Data: The datasets generated during and/or analyzed during the current study are not publicly available because the Research Ethics Committee of Wakayama Medical University must understand the actual use of the datasets but are available from the corresponding author upon reasonable request.

References

1. Soroceanu A, Diebo BG, Burton D, et al. Radiographical and implant-related complications in adult spinal deformity surgery: incidence, patient risk factors, and impact on health-related quality of life. *Spine* 2015;40(18):1414-21.
2. Yagi M, Akilah KB, Boachie-Adjei O. Incidence, risk factors and classification of proximal junctional kyphosis: surgical outcomes review of adult idiopathic scoliosis. *Spine* 2011;36(1):E60-8.
3. Kim YJ, Bridwell KH, Lenke LG, et al. Proximal junctional kyphosis in adult spinal deformity after segmental posterior spinal instrumentation and fusion: minimum five-year follow-up. *Spine* 2008;33(20):2179-84.
4. Lee JH, Kim JU, Jang JS, et al. Analysis of the incidence and risk factors for the progression of proximal junctional kyphosis following surgical treatment for lumbar degenerative kyphosis: minimum 2-year follow-up. *Br J Neurosurg* 2014;28(2):252-8.
5. Alentado VJ, Lubelski D, Healy AT, et al. Predisposing characteristics of adjacent segment disease after lumbar fusion. *Spine* 2016;41(14):1167-72.
6. Hilibrand AS, Robbins M. Adjacent segment degeneration and adjacent segment disease: the consequences of spinal fusion? *Spine J* 2004;4(6):190S-4S.
7. Hamilton DK, Buza JA III, Passias P, et al. The fate of patients with adult spinal deformity incurring rod fracture after thoracolumbar fusion. *World Neurosurg* 2017;106:905-11.
8. Luo M, Wang P, Wang W, et al. Upper thoracic versus lower thoracic as site of upper instrumented vertebrae for long fusion surgery in adult spinal deformity: a meta-analysis of proximal junctional kyphosis. *World Neurosurg* 2017;102:200-8.
9. Lertudomphonwanit T, Kelly MP, Bridwell KH, et al. Rod fracture in adult spinal deformity surgery fused to the sacrum: prevalence, risk factors, and impact on health-related quality of life in 526 patients. *Spine J* 2018;18(9):1612-24.
10. Watanabe K, Lenke LG, Bridwell KH, et al. Proximal junctional vertebral fracture in adults after spinal deformity surgery using pedicle screw constructs: analysis of morphological features. *Spine* 2010;35(2):138-45.
11. Etebar S, Cahill DW. Risk factors for adjacent-segment failure following lumbar fixation with rigid instrumentation for degenerative instability. *J Neurosurg* 1999;90(2):163-9.
12. Toyone T, Ozawa T, Kamikawa K, et al. Subsequent vertebral fractures following spinal fusion surgery for degenerative lumbar disease: a mean ten-year follow-up. *Spine (Phila Pa 1976)* 2010;35(21):1915-8.
13. Hassanzadeh H, Gupta S, Jain A, et al. Type of anchor at the proximal fusion level has a significant effect on the incidence of proximal junctional kyphosis and outcome in adults after long posterior spinal fusion. *Spine Deform* 2013;1(4):299-305.
14. Helgeson MD, Shah SA, Newton PO, et al. Evaluation of proximal junctional kyphosis in adolescent idiopathic scoliosis following pedicle screw, hook, or hybrid instrumentation. *Spine* 2010;35(2):177-81.
15. Line BG, Bess S, Lafage R, et al. Effective prevention of proximal junctional failure in adult spinal deformity surgery requires a combination of surgical implant prophylaxis and avoidance of sagittal alignment overcorrection. *Spine* 2020;45(4):258-67.
16. Hackenberg L, Link T, Liljenqvist U. Axial and tangential fixation strength of pedicle screws versus hooks in the thoracic spine in relation to bone mineral density. *Spine* 2002;27(9):937-42.
17. Cordista A, Conrad B, Horodyski M, et al. Biomechanical evaluation of pedicle screws versus pedicle and laminar hooks in the thoracic spine. *Spine J* 2006;6(4):444-9.
18. Tsutsui S, Hashizume H, Yukawa Y, et al. Optimal anchor at the uppermost instrumented vertebra in long fusion from the pelvis to the lower thoracic spine in elderly patients with degenerative spinal deformity: hook versus pedicle screw. *Clin Spine Surg* 2022;35(1):E280-4.
19. Kozaki T, Tsutsui S, Yamamoto E, et al. Quantitative biomechanical evaluation for optimal spinal instrumentation to prevent mechanical complications in spinal fusion from the lower thoracic spine to the pelvis for adult spinal deformity: a finite element analysis. *Spine Surg Relat Res* 2023;7(3):276-83.
20. Lubelski D, Healy AT, Mageswaran P, et al. Biomechanics of the lower thoracic spine after decompression and fusion: a cadaveric analysis. *Spine J* 2014;14(9):2216-23.
21. Harrington PR. Treatment of scoliosis. Correction and internal fixation by spine instrumentation. *J Bone Joint Surg Am* 1962;44(4):591-634.
22. Yazici M, Asher MA, Hardacker JW. The safety and efficacy of

- Isola-Galveston instrumentation and arthrodesis in the treatment of neuromuscular spinal deformities. *J Bone Joint Surg Am* 2000;82(4):524-43.
23. Imai K, Ohnishi I, Bessho M, et al. Nonlinear finite element model predicts vertebral bone strength and fracture site. *Spine* 2006;31(16):1789-94.
 24. Keyak JH, Rossi SA, Jones KA, et al. Prediction of femoral fracture load using automated finite element modeling. *J Biomech* 1998;31(2):125-33.
 25. Phillips AT, Pankaj P, Howie CR, et al. Finite element modelling of the pelvis: inclusion of muscular and ligamentous boundary conditions. *Med Eng Phys* 2007;29(7):739-48.
 26. Goel VK, Kim YE, Lim TH, et al. An analytical investigation of the mechanics of spinal instrumentation. *Spine* 1988;13(9): 1003-11.
 27. Shi D, Wang F, Wang D, et al. 3-D finite element analysis of the influence of synovial condition in sacroiliac joint on the load transmission in human pelvic system. *Med Eng Phys* 2014;36(6): 745-53.
 28. Yamamoto I, Panjabi MM, Crisco T, et al. Three-dimensional movements of the whole lumbar spine and lumbosacral joint. *Spine* 1989;14(11):1256-60.
 29. Han S, Hyun SJ, Kim KJ, et al. Rod stiffness as a risk factor of proximal junctional kyphosis after adult spinal deformity surgery: comparative study between cobalt chrome multiple-rod constructs and titanium alloy two-rod constructs. *Spine J* 2017;17(7):962-8.
 30. Hirano T, Hasegawa K, Takahashi HE, et al. Structural characteristics of the pedicle and its role in screw stability. *Spine* 1997;22(21):2504-9.
 31. Zdeblick TA, Kunz DN, Cooke ME, et al. Pedicle screw pullout strength. Correlation with insertional torque. *Spine* 1993;18(12): 1673-6.
 32. Zindrick MR, Wiltse LL, Widell EH, et al. A biomechanical study of intrapeduncular screw fixation in the lumbosacral spine. *Clin Orthop Relat Res* 1986;203:99-112.
 33. Brantley AG, Mayfield JK, Koeneman JB, et al. The effects of pedicle screw fit. An in vitro study. *Spine* 1994;19(15):1752-8.
 34. Coe JD, Warden KE, Herzig MA, et al. Influence of bone mineral density on the fixation of thoracolumbar implants. A comparative study of transpedicular screws, laminar hooks, and spinous process wires. *Spine* 1990;15(9):902-7.
 35. Hohn EA, Chu B, Martin A, et al. The pedicles are not the densest regions of the lumbar vertebrae: implications for bone quality assessment and surgical treatment strategy. *Global Spine J* 2017;7(6):567-71.
 36. Wang Y, Videman T, Boyd SK, et al. The distribution of bone mass in the lumbar vertebrae: are we measuring the right target? *Spine J* 2015;15(11):2412-6.
 37. Doodkorte RJP, Vercoulen TFG, Roth AK, et al. Instrumentation techniques to prevent proximal junctional kyphosis and proximal junctional failure in adult spinal deformity correction-a systematic review of biomechanical studies. *Spine J* 2021;21(5):842-54.
 38. Hasegawa K, Takahashi HE, Uchiyama S, et al. An experimental study of a combination method using a pedicle screw and laminar hook for the osteoporotic spine. *Spine* 1997;22(9):958-62; discussion 963.
 39. Tanouchi T, Shimizu T, Fueki K, et al. Adjacent-level failures after occipito-thoracic fusion for rheumatoid cervical disorders. *Eur Spine J* 2014;23(3):635-40.
 40. Tanouchi T, Shimizu T, Fueki K, et al. Distal junctional disease after occipitocervical fusion for rheumatoid cervical disorders: correlation with cervical spine sagittal alignment. *Global Spine J* 2015;5(5):372-7.
 41. Kozaki T, Kozaki T, Nagata K, et al. Dynamic cord compression induced by proximal junctional failure and loose pedicle screws after thoracolumbar fusion surgery: a case report. *BMC Musculoskelet Disord* 2023;24(1):669.
 42. Bruno AG, Burkhardt K, Allaire B, et al. Spinal loading patterns from biomechanical modeling explain the high incidence of vertebral fractures in the thoracolumbar region. *J Bone Miner Res* 2017;32(6):1282-90.
 43. Sales de Gauzy J, Jouve JL, Ilharreborde B, et al. Use of the universal Clamp in adolescent idiopathic scoliosis. *Eur Spine J* 2014; 23 Suppl 4:S446-51.
 44. La Rosa G, Giglio G, Oggiano L. The universal clamp hybrid system: a safe technique to correct deformity and restore kyphosis in adolescent idiopathic scoliosis. *Eur Spine J* 2013;22(Suppl 6): S823-8.
 45. La Rosa G, Giglio G, Oggiano L. Surgical treatment of neurological scoliosis using hybrid construct (lumbar transpedicular screws plus thoracic sublaminar acrylic loops). *Eur Spine J* 2011;20(Suppl 1):S90-4.
 46. Tsutsui S, Yamamoto E, Kozaki T, et al. Biomechanical study of rod stress in lumbopelvic fixation using lateral interbody fusion: an in vitro experimental study using synthetic bone models. *J Neurosurg Spine* 2022;37(1):7.
 47. Buyuk AF, Dawson JM, Yakel S, et al. Does pelvic incidence tell us the risk of proximal junctional kyphosis in adult spinal deformity surgery? *Eur Spine J* 2022;31(6):1438-47.

Spine Surgery and Related Research is an Open Access journal distributed under the Creative Commons Attribution-NonCommercial-NoDerivatives 4.0 International License. To view the details of this license, please visit (<https://creativecommons.org/licenses/by-nc-nd/4.0/>).